Abstract

The dynamic behaviour of short simply-supported railway bridges under convoy circulations and, especially, the effect of soil structure interaction (SSI) in the maximum expectable deck transverse response is the aim of this study. These structures due to their usually light weight may experience excessively high acceleration levels under resonant conditions. In order to approach this wave propagation problem, a coupled three-dimensional Boundary Element-Finite Element model formulated in the time domain is used to reproduce the soil and structural behaviour, respectively. As the resonant phenomenon in this application is highly influenced by the free vibration response of the deck, a sensitivity analysis is designed in order to first analyse how SSI affects the free vibration response of beams under the circulation of a single moving load in a wide range of velocities. A subset of beam bridges is defined considering span lengths ranging from 12.5 to $25\,\mathrm{m}$, and fundamental frequencies covering associated typologies. A single soil layer is considered with shear wave velocities ranging from 150 to $365\,\mathrm{m/s}$. From the single load free vibration parametric analysis conclusions are derived regarding the conditions of maximum free vibration and cancellation of the response. These conclusions are used afterwards to justify how resonant amplitudes of the bridge under the circulation of railway convoys are affected by the soil properties, leading to substantially amplified responses or to almost cancelled ones, and numerical examples are included to show the aforementioned situations.

Keywords: railway bridges, soil-structure interaction, resonance, cancellation, moving loads, BEM-FEM coupled model.

1 Introduction

As modern railway transportation systems become faster and heavier, imposing more and more demanding requirements on the infrastructures, it becomes essential to improve the understanding and the capability to predict the dynamic response of bridges under railway traffic, especially with the advent of High-Speed. In this context, the dynamic response of beams under the circulation of moving loads has been a deeply investigated topic during the last decades [1, 2, 3, 4, 5, 6]. Railway bridges have received special attention in the structural dynamics context as the periodic nature of axle loads may induce important vibration levels in the structures, particularly under resonant conditions [7]. Especially critical in this regard are short-to-medium span bridges composed by simply-supported (S-S) decks with usually low associated masses (see Figure 1), which may experience high levels of transverse accelerations in these situations. This problem aggravates for low structural damping levels, typical in the aforementioned constructions [7]. Resonance in railway bridges may lead to adverse consequences such as ballast destabilization, general degradation of the track and a raise in the maintenance costs of the line.

Figure 1: Railway bridge in High Speed line composed by short simply supported bays

Resonance in S-S bridges takes place when the excitation period of the axles, i.e. the ratio between the characteristic distance, or distance causing resonance, and the train speed, is a multiple of one of the structure's natural periods. When this occurs, the free vibration oscillations induced on the structure when each load abandons it accumulate, and the transverse response of the bridge progressively increases if the number of axles is sufficient. In short to medium span bridges with nowadays maximum train speeds, the characteristic distance associated with detrimental levels of transverse accelerations due to resonance usually corresponds to the length of the passengers' coaches. Therefore, the amplification of the transverse response of beams or bridges at resonance depends both on the periodicity of the loads and on the amplitude of the free vibrations left by every single load. Under ideal S-S conditions and in the absence of damping, the amplification of the free vibrations left by the circulation of

a single load depends on the ratio between the travelling speed and the structural frequencies, as this governs the appearance of maximum free vibrations or cancellation situations [8].

Studies on resonance and cancellation in beams under moving loads have been reported in the past years. Pesterev et al. [9] predicted the travelling speeds leading to minimum levels of free vibration in SS beams. Yang et al. [10] analysed the suppression of the beam first resonance for certain span to car length ratios. Museros et al. [8] predicted the maximum free vibration and cancellation conditions of S-S and elastically-supported (E-S) beams under a single load, and explained on this basis the maximum resonance and cancellation of resonance phenomena. Yang [11] analysed the resonant and cancellation speeds of E-S beams and compared them with those of the S-S case. He concluded that the resonant speed reduces with the flexibility of the supports, but the cancellation velocity is not much affected. Other recent studies on the resonance and cancellation mechanisms on simply and elastically supported beams may be found in [12, 13, 14]. Generally speaking, the free vibration levels of beams or bridges under moving loads, and their effect on the amplification or cancellation of resonance have been evaluated in the past considering simple models for the bridge structure: generally SS beams, ES beams, and SS or ES plates [15, 16], when the contribution of three-dimensional deformation modes of the deck needs to be considered. In all these studies, the soil-structure interaction (SSI) effect is neglected.

Only a few authors have investigated the dynamic response of beams or bridges taking into account the radiation of the waves transmitted through the soil. According to some authors in certain soil environments, an increase in the fundamental natural period of moderately flexible structures due to SSI may have a detrimental effect on the structural behaviour [17].

A concise review on the historical evolution of the soil-structure interaction field may be found in [18]. For the application of railway bridge structures, which is the object of this investigation, some authors [19, 20, 21] suggest that the resonant response of a railway bridge could be considerably affected by the soil flexibility, leading to a reduction of the resonant speeds and of the transverse response amplitudes at the deck level due to the increase of damping. Ülker-Kaustell et al. [19] presented a qualitative analysis of the dynamic SSI of a portal frame railway bridge based on dynamic stiffness functions. The authors studied train-bridge resonance of the bridge model using a direct integration method. The authors concluded that the contribution to the modal damping ratios of the coupled soil-bridge system was substantial, especially for the lower range of the soil elastic modulus, and this effect could resolve the situation in which the designer cannot meet the requirements on deck vertical acceleration according the design code. Romero et al. [20] also studied the dynamic soil-bridge interaction in high speed railway lines. The analysis was conducted using a general and fully three-dimensional multi-body boundary element-finite element (BEM-FEM) model formulated in the time domain. The authors concluded that SSI affected the structure dynamic behaviour: the fundamental periods and damping ratios of the response were higher when SSI was considered. Ju [21] developed a FE model

including the effect of SSI to calculate railway bridge natural frequencies. The FE model included bridge girders, piers, foundations, soil, and water. The calculated natural frequencies taking into account the fluid-structure interaction effect were always lower than in the absence of it.

In the opinion of the authors of this contribution, there is a need to understand how SSI effects affect the free vibration response of beams, and the maximum free vibration and cancellation phenomena, which are the fundamental aspects governing resonance. Moreover, this study should be carried out considering different bridge lengths and deck typologies in order to be able to obtain general trends and conclusions. The present contribution shows the main parameters that govern the SSI effects in this regard and the fundamental trends in the evolution of the bridge resonant response with them.

2 Formulation and approach adopted for the analysis

2.1 Approach of the investigation

The objective of the investigation is to evaluate the SSI effects on the transverse response of beams traversed by moving loads at constant speeds. First the structure response will be analysed under the circulation of a single load in a wide range of velocities in order to determine the conditions for maximum response and cancellation of the response during the free vibration phase (once the load has left the structure). This relates with the amplification of resonance and cancellation of resonance that may occur when the beam is subjected to trains of equidistant loads at certain speeds. Museros et al. [8] investigated this phenomenon solving the analytical conditions for maximum free vibration response and cancellation in simply-supported and elastically-supported beams (Figure 2) and stated that these conditions, when coincide with resonant velocities, provoke very relevant resonant amplifications or almost inexistent resonant situations.

In this study a numerical method based on a three dimensional (3D) boundary element-finite element coupled formulation in time domain [22] is used to analyze the importance of the free vibration amplitudes in the resonant response of beams and bridges. The proposed model allows to study soil-structure interaction by domain decomposition in two subdomains represented by the BEM and the FEM. Soil behaviour is represented by the BEM, and the radiation condition is implicitly satisfied in the fundamental solution. This work uses the half-space Green's functions, considering the internal soil damping directly in the time domain formulation [23]. The structures are modelled with the FEM. A discretization example of the coupled BEM-FEM model used in this paper to analyse SSI effects is represented in Figure 3.

In a first approximation, a beam FEM is used to represent the deck flexural behaviour under moving loads, assuming therefore that the deck vertical response is mainly governed by the contribution of longitudinal bending modes. The beam end

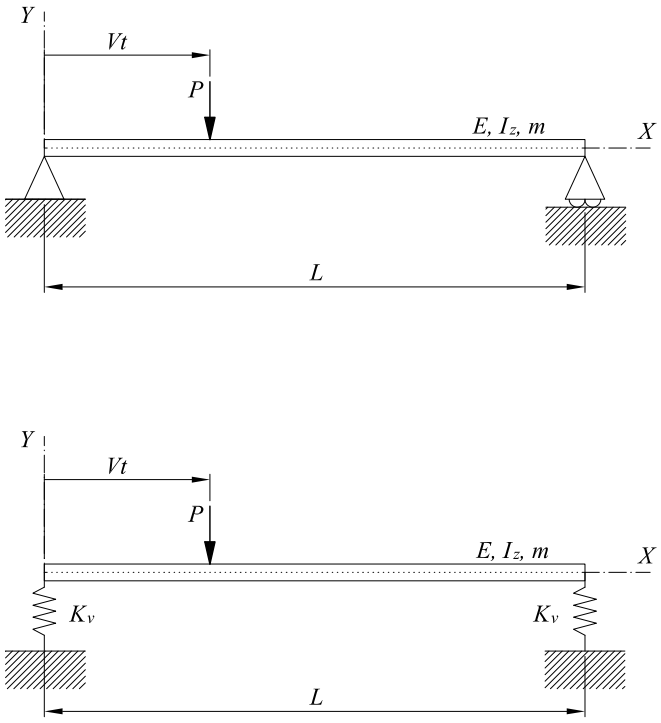

Figure 2: Schematic representation of a simply supported and elastically supported beam under travelling load

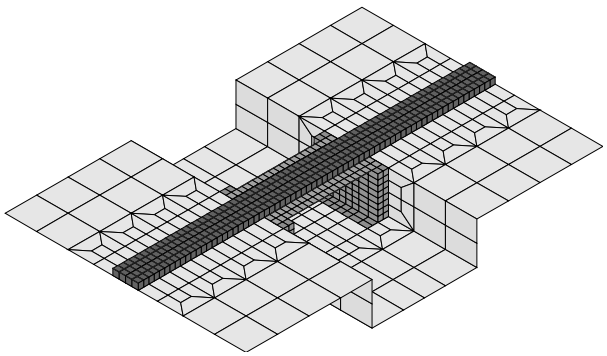

Figure 3: Discretization example of a coupled BEM-FEM for SSI analysis

sections are connected through kinematic constraints to two rigid plates representing in a first approach and simple approximation the lower surface of the shallow foundations at the abutments. These plates are coupled to the BEs simulating the interaction with the soil. The described model is represented in 4.

The detailed geometry of the substructure has not been included in this investigation for the following reasons: (1) the main objective is to detect the fundamental parameters that affect the SSI effects on the bridge deck resonant response and evaluate the main tendencies of these parameters; (2) an exhaustive parametric analysis is per-

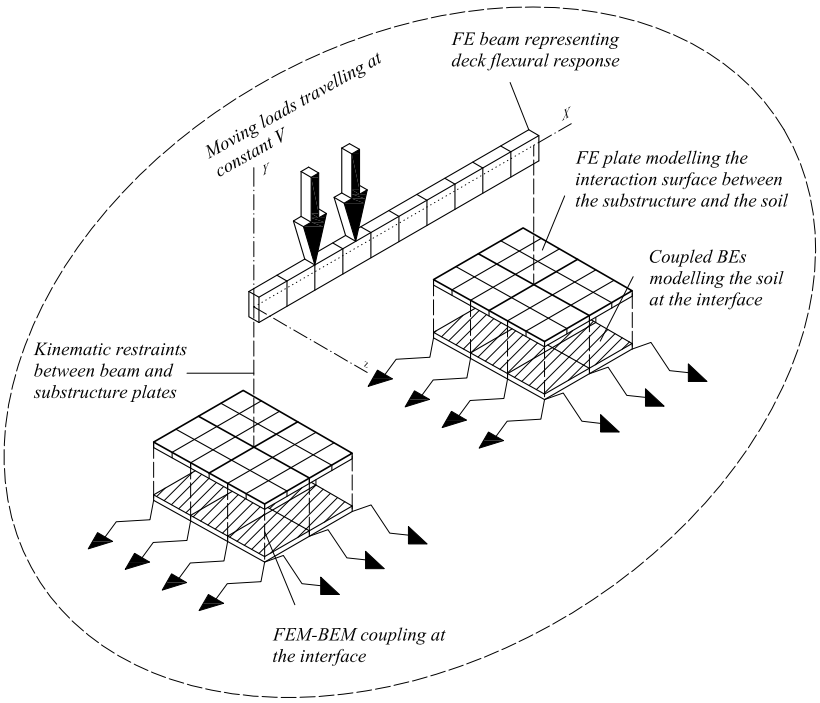

Figure 4: Schematic representation of the model under analysis

formed in what follows considering a wide range of circulating velocities, structural and soil properties, entailing considerably high computational times; (3) the fundamental effects of SSI on the resonant response of bridge decks have not been analysed before covering the proposed factors. As the investigation if focused on the superstructure response, and not on the substructure, the authors have preferred to keep the foundations geometry as simple as possible in order to isolate the essence of the wave propagation problem and evaluate its influence on the bridge vibration response [24].

2.2 Mathematical model

The BEM is based on a time marching procedure to obtain the time variation of the boundary unknowns; i.e. displacements and tractions. The $k-th$ component for displacements and tractions over the boundary are approximated from their nodal values j at each time step m, u_k^{mj} and p_k^{mj}, using the space interpolation functions $\phi^j(r)$ and $\psi^j(r)$. After interpolating the boundary variables, the integral representation of the displacement u at a point i on the boundary becomes [25]:

$$c_{lk}^{i}u_{k}^{i}(\mathbf{x}^{i},t)=\sum_{m=1}^{n}\sum_{j=1}^{Q}\left\{\left[\int_{\Gamma_j}U_{lk}^{nm}\psi^{j}\,d\Gamma\right]p_{k}^{mj}-\left[\int_{\Gamma_j}P_{lk}^{nm}d\tau\phi^{j}\,d\Gamma\right]u_{k}^{mj}\right\} \tag{1}$$

where Q is the total number of boundary nodes and Γ_j represents the elements to which node j belongs. Time kernels U_{lk}^{nm} and P_{lk}^{nm} are respectively computed through the fundamental solution for displacements and tractions due to a point load at $\mathbf{x}^i$ acting in the l direction. These kernels are analytically integrated by parts using constant and linear piecewise time interpolation functions for tractions and displacements [23], respectively. Equation (1) is written in a more compact form as:

$$c_{lk}^{i}u_{k}^{ni}=\sum_{m=1}^{n}\sum_{j=1}^{Q}\left[G_{lk}^{nmij}p_{k}^{mj}-\widehat{H}_{lk}^{nmij}u_{k}^{mj}\right] \tag{2}$$

Once the integral-free term c_{lk}^{i} is included in the system matrix, the integral representation for point i at time $t=n\Delta t$ becomes:

$$\mathbf{H}^{nn}\mathbf{u}^{n}=\mathbf{G}^{nn}\mathbf{p}^{n}+\sum_{m=1}^{n-1}\left[\mathbf{G}^{nm}\mathbf{p}^{m}-\mathbf{H}^{nm}\mathbf{u}^{m}\right] \tag{3}$$

where H_{lk}^{nmij} collects for c_{lk}^{i} when $i=j$ and $n=m$.

The FEM equation at time step n is defined as [26]:

$$\mathbf{M}\ddot{\mathbf{u}}^{n}+\mathbf{C}\dot{\mathbf{u}}^{n}+\mathbf{K}\mathbf{u}^{n}=\mathbf{f}^{n} \tag{4}$$

where **M**, **C** y **K** are mass, damping, and stiffness matrices, respectively. $\mathbf{u}^n$, $\dot{\mathbf{u}}^n$ y $\ddot{\mathbf{u}}^n$ represent nodal displacement, velocity, and acceleration vectors, respectively, and $\mathbf{f}^n$ is the load vector.

Equation 4 is solved using an implicit time integration GN22 Newmark method [26, 27]. An equivalent dynamic stiffness matrix is defined:

$$\mathbf{D}\mathbf{u}^{n}=\mathbf{f}^{n}+\mathbf{f}^{n-1} \tag{5}$$

Coupling of BEM and FEM (Equations 3 and 5) is carried out by imposing equilibrium and compatibility conditions at the soil-structure interface. Both systems of equations are assembled into a single global system, together with the equilibrium and compatibility equations [28].

Under the assumption that plate foundations behave as rigid bodies, the BEM Equation (3) is expressed in terms of the kinematic constraint matrix **L** relating mid-point plate displacement with any other point for each foundation:

$$\mathbf{H}^{nn}\mathbf{Lu}^{n} = \mathbf{G}^{nn}\mathbf{LTp}^{n} + \sum_{m=1}^{n-1}\left[\mathbf{G}^{nm}\mathbf{LTp}^{m} - \mathbf{H}^{nm}\mathbf{Lu}^{m}\right] \tag{6}$$

where equilibrium of forces at the interface Γ is fulfilled integrating nodal tractions according to the element shape function $\mathbf{N}$:

$$\mathbf{f} = \int_{\Gamma} \mathbf{N}^{T}\mathbf{pN}\, d\Gamma = \mathbf{Tp} \tag{7}$$

The time step Δt for the analysis was set to properly represent the structure dynamic behaviour and the load excitation. Both criterion defines the following constraint:

$$\Delta t = \min\left(\frac{2\pi}{\omega_1 k_\omega}, \frac{L_p}{v k_v}\right) \tag{8}$$

where ω_1 corresponds to the first resonant angular frequency of the structure, L is the bridge length, and V is the load speed. Parameters k_ω and k_v define time discretizations for the structure fundamental period and the load passage time, respectively, and both take a value of 60 time steps.

The chosen time step determines the spatial boundary element discretization according with the stability parameter $\beta = c_s \Delta t / \Delta l$, where l is the distance between two nodes of a boundary element, and c_s is the shear wave propagation velocity in the soil. In this work, a stability parameter equals $\beta = 0.5$ has been considered.

The finite element representation is determined by the bridge bending wavelength discretization. Minimum wavelength is defined by the maximum frequency range and the phase bending wave propagation velocity $c_B = \sqrt[4]{\omega_1^2 EI/m_b}$, where EI is the bridge bending stiffness, m_b is the bridge mass per unit length, and ω_1 is the first mode angular frequency. This paper considers 20 element for the minimum wavelength.

This work uses the `SSIFiBo` toolbox for `MATLAB` previously developed by Galvín and Romero [22, 25, 29]. The FEM module of the toolbox does not include any preprocessor. Instead, a gateway for commercial software allows importing directly the structure model.

2.3 Definition of the sensitivity analysis

In order to be able to derive general conclusions applicable to different bridge lengths, deck typologies, soil properties and circulating velocities, an extensive parametric numerical study is designed. Beams of lengths ranging from 12.5 to $25\,\mathrm{m}$ in increments of length of $2.5\,\mathrm{m}$ are considered. For each length, three theoretical fundamental frequencies, covering the Eurocode 1 frequency range for dynamic simplified analysis [30] of simply-supported railway bridges are selected (see Figure 5). In what follows $f_{1,000}$, $f_{1,100}$ and $f_{1,050}$ stand for the Eurocode 1 fundamental frequency lower limit, upper limit and mean value for each length considered. Beam masses have been assigned in order to represent realistic deck typologies found in

conventional and High-Speed lines structures, after the studies from [31]. In particular linear deck masses of $m_b = L(m) \cdot 1000\,\mathrm{kg/m^2}$ are considered for each length. Regarding the soil properties, four single layer soil types are defined with flexibilities covering the AASHTO classification [32], in particular with s and p-wave velocities of $c_s = \{365, 220, 150, 80\}\ \mathrm{m/s}$ and $c_p = 2c_s$. Soil density has been set equal to $1800\,\mathrm{kg/m^3}$. Regarding structural damping, in a first approach the study is performed without structural damping. No material damping is assigned to the soil either. Eliminating damping permits a better comparison of cancellation conditions with the analytical solution of the elastically-supported beam. In the numerical examples presented in section 4, Rayleigh damping is assigned to the bridge structure.

Two types of analyses are performed and presented in this section for all the bridge-soil combinations under study: (i) identification of fundamental frequencies and (ii) dynamic time-history analysis under the circulation of single axle load travelling at constant speed. The circulating velocities of the load are included in the following interval, expressed in terms of the non-dimensional speed parameter K_1 associated to the fundamental mode:

$$K_1 = \frac{V\pi}{L\omega_1} \in [0.1, 0.5] \tag{9}$$

where ω_1 is the fundamental frequency of the beam. The 0.5 limit is above the highest speeds that can be reached nowadays with existing rolling stock and railway infrastructures.

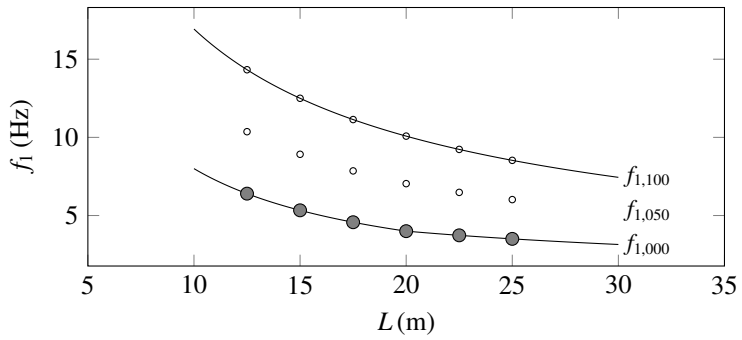

Figure 5: Eurocode 1 [30] lower and upper frequency limits for simplified dynamic analysis. Circles: reference bridges under study

3 Sensitivity analysis results

3.1 Modal identification of the bridges under study

First the fundamental natural frequencies of 72 bridges (6 lengths $\cdot$ 3 frequencies $\cdot$ 4 soil types) under study considering SSI have been identified from the response under

impulse loading. Figure 6 shows the evolution of the frequencies with the soil flexibility. In the vertical axis the fundamental frequency computed considering SSI has been divided by that of the infinitely rigid soil (S-S case). In the plot, three lengths are included (12.5, 17.5 and $25\,\mathrm{m}$) for the sake of clarity, as intermediate lengths show a comparable evolution.

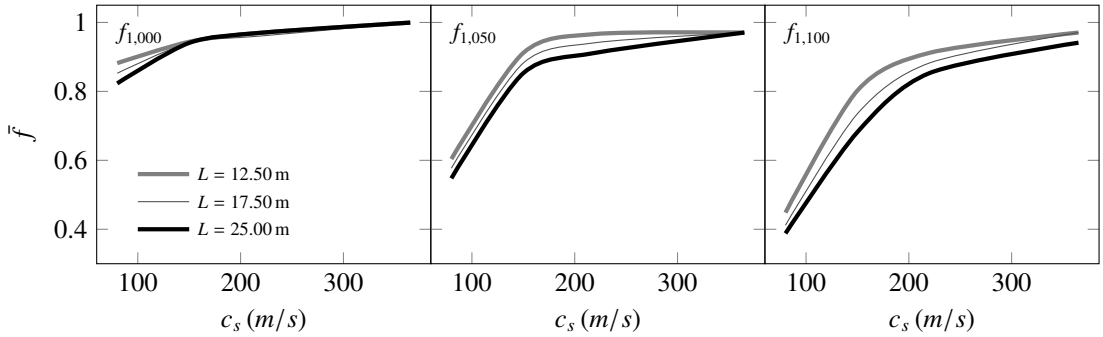

Figure 6: Evolution of the bridge fundamental frequencies with soil flexibility

As c_s increases, and therefore the soil becomes stiffer, the fundamental frequency of the beams tends to that of the SS case. The structures that are less affected by the soil flexibility are those with lower natural frequency for all the lengths ($f_{1,000}$ stands for the lower frequency limit in Figure 5). These beams fundamental frequency is reduced around 20% for the most flexible soils and the longest spans. Bridges with highest natural frequencies ($f_{1,100}$, upper limit in Figure 5) are most affected by the SSI effects, experiencing maximum reductions in the fundamental frequency that reach 50% in the softer soils. It must be clarified that $c_s = 80\,\mathrm{m/s}$, most flexible soil under consideration in the modal identification, is a considerably soft soil, but it has been included in this section in order to point out the interaction effect. These results are consistent with the frequency evolution included in [8] for the ES beam. In this contribution it was shown that natural frequencies were more affected as the ratio between the supports flexibility and the structure flexural flexibility increased. As all the beams with the same length present the same mass, lower frequencies entail more flexible structures as well.

3.2 Maximum free vibration response under a single moving load

In this section the maximum response of the beams in the free vibration phase left by the circulation of a single load is evaluated. In Figures 7 and 8 the maximum transverse displacement at mid-span, non-dimensionalized by the static deflection, R, computed in the free vibration phase (once the load has left the beam) is represented for bridges with the lowest natural frequencies (those marked as $f_{1,000}$ in Figure 5) in terms of the circulating velocity. Figures 7a and 8a show the analytical solution for the ES beam (Figure 2), included in [8]. In particular R_1 stands for the maximum transverse response associated to the fundamental mode of the E-S beam divided by

the static solution; and κ is the ratio between the supports vertical flexibility and the beam flexural flexibility (κ=0 corresponds to the S-S case). In figures 7b to 7d and 8b to 8d the dynamic response of the BEM-FEM bridge model has been represented for values of $L = 12.5$, 15 and $17.5\,\mathrm{m}$ and $L = 20$, 22.5 and $25\,\mathrm{m}$, respectively. Both the analytical ES response and the numerical one have been computed in the absence of damping, in order to be able to visualize more clearly the evolution of the cancellation conditions.

From the analysis of figures 7 and 8 several aspects should be pointed out: (i) when the SSI is taken into account velocities leading to maximum free vibration response and to cancellation sequentially take place, in the same way that occurs for the E-S beam; (ii) as c_s and c_p decrease, going from stiffer to softer soils, the cancellation non-dimensional velocities increase as in the E-S case. This is related with the alteration in the beams natural frequencies only due to the soil effect. In fact cancellation linear velocities remain unmodified with the flexibility of the soil (this phenomenon is consistent with the works of [8]); (iii) in the plot, depending on the non-dimensional speed interval, the maximum free vibration response may be associated to stiffer or softer soils; (iv) even though for the SSI problem the response is obtained with the full model, and it is not limited to the fundamental modal response as in 7a and 8a, cancellation takes place at certain speeds and the response in free vibration practically vanishes; (v) when the beam transverse response is represented as a nondimensional magnitude (R) in terms of the nondimensional velocity (K_1), the maximum free vibration and cancellation conditions are practically not affected by the beam length.

The practical application of these results is that conclusions regarding the type of resonant response to be expected when the same structure is subjected to the circulation of a train of loads (instead of a single axle) may be drawn. In particular if a resonant velocity is close to a cancellation speed the resonant amplitude will drastically reduce and may practically be imperceptible. On the other hand, if the resonant velocity takes place close to a maximum free vibration condition the amplification should be substantial. In the following section a few cases of particular bridges subjected to resonance are presented to show the aforementioned situations.

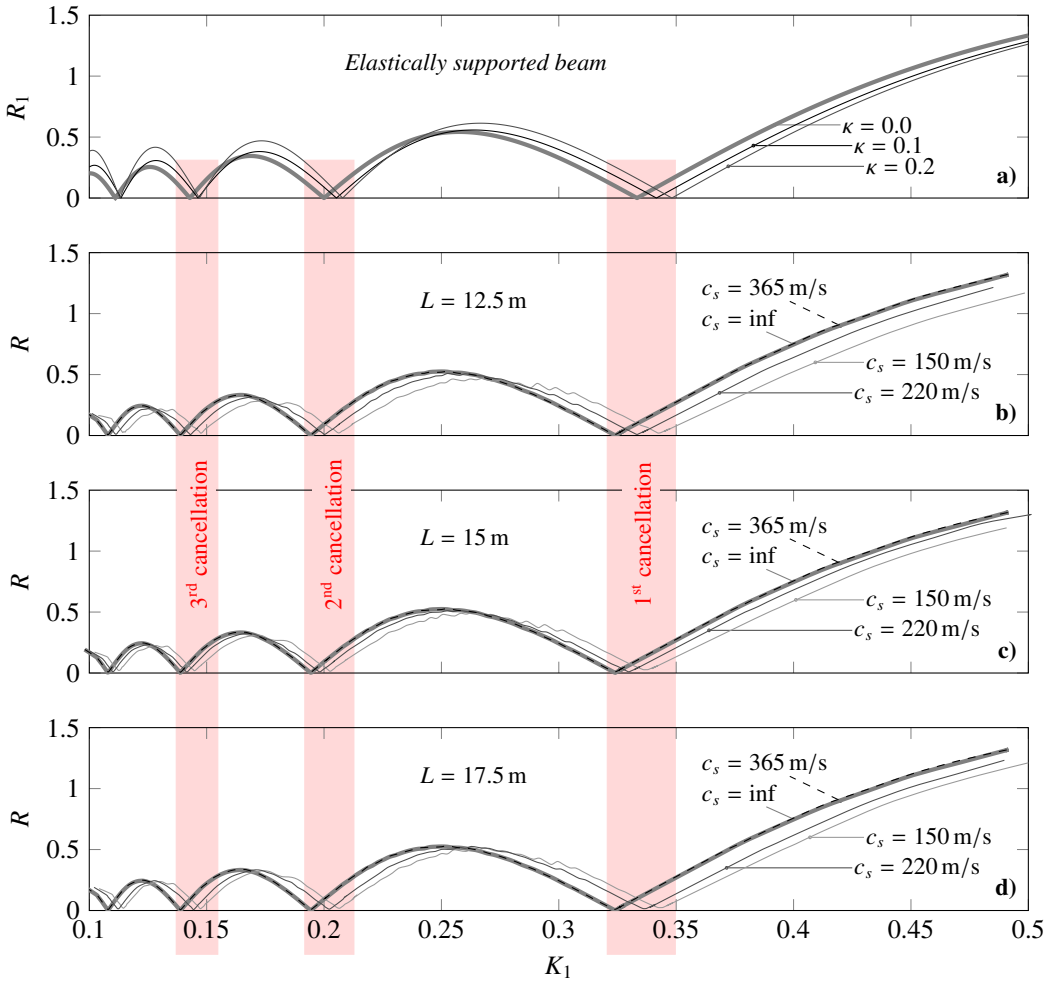

Figure 7: Maximum free vibration displacement response of (a) elastically-supported beam; and (b)-(d) BEM-FEM model with $L = 12.5 - 17.5\,\mathrm{m}$ and $f_{1,000}$ under constant moving force including SSI ($\zeta_b = 0$, $\zeta_s = 0$)

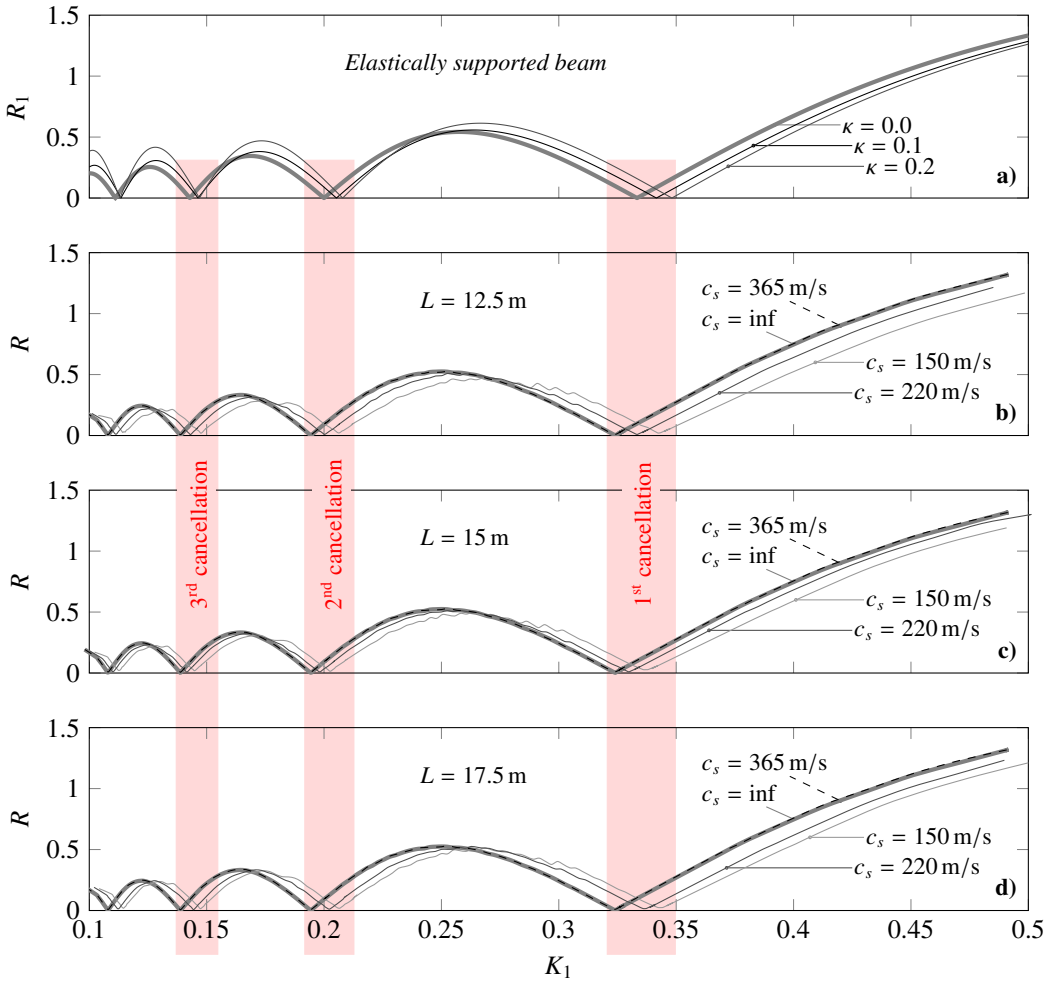

Figure 8: Maximum free vibration displacement response of (a) elastically-supported beam; and (b)-(d) BEM-FEM model with $L = 20 - 25\,\mathrm{m}$ and $f_{1,000}$ under constant moving force including SSI ($\zeta_b = 0$, $\zeta_s = 0$)

4 Case studies

In this section a bridge of $12.5\,\mathrm{m}$ span length is analysed under the circulation of trains of constant loads in order to provide some examples of the main conclusions extracted after the sensitivity analyses.

Two types of train models are considered: the HSLM-A model from Eurocode 1 [30], which is a train composed by equidistant pairs of loads, and a hypothetical equidistant load train. Both models are shown in Figure 9. In Table 1 the particular parameters that define the four trains that are used in the following examples are included, where N stand for the number of passenger coaches, d for the characteristic distance of the train (or distance causing resonance) and P for the load value per axle.

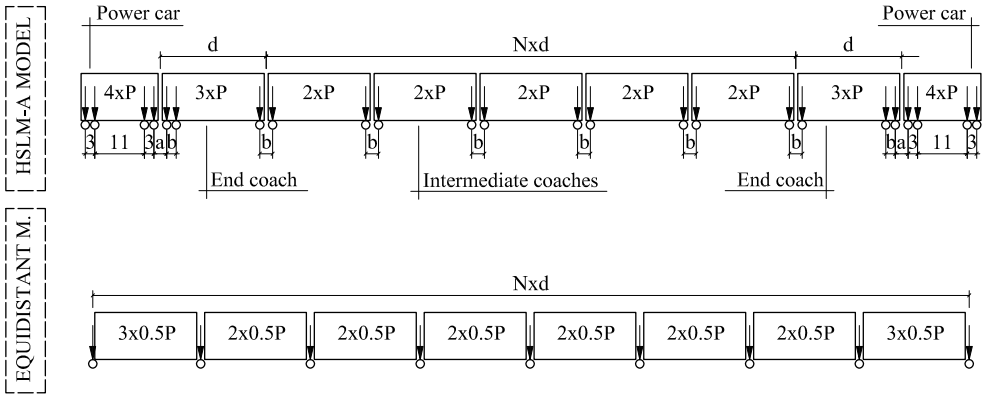

Figure 9: HSLM-A and equidistant train load schemes

Train name	Type name	N	$a\,(\mathrm{m})$	$b\,(\mathrm{m})$	$d\,(\mathrm{m})$	$P\,(\mathrm{kN})$
A5	HSLM-A	14	3.525	2	22	170
A7	HSLM-A	13	3.525	3	24	190
A30	Equidistant	49	—	—	16.675	170
A31	Equidistant	49	—	—	16.200	170

Table 1: Train load models definition

4.1 Cancellation of resonance considering SSI

In the following example the $12.5\,\mathrm{m}$ length bridge with the lowest natural frequency, $f_{1,000}$, is considered in the S-S case (neglecting SSI effects) and including SSI with $c_s = 220\,\mathrm{m/s}$. In both cases a second resonance of the bridge fundamental mode is forced in two scenarios: (a) the resonant velocity coincides with a cancellation condition; and (b) the second resonance does not coincide with a cancellation condition. A suitable train is selected to force these two situations. The condition for a second resonance to be cancelled occurs when:

$$V_{2nd,res} = \frac{df_1}{2} = \frac{K^i_{1,\text{canc}} L \omega_1}{\pi} \rightarrow d = 4K_{1,\text{canc}} L \tag{10}$$

where i is the cancellation order. The first cancellation for the second resonance of this particular structure takes place for when $c_s = 220\,\mathrm{m/s}$ and for infinitely rigid soil (see Figure 7b). For these values the characteristic distances of the trains leading to cancellation of the beam second resonance are computed, along with the resonant velocity (same in both cases due to the alteration in both the cancellation condition and the bridge natural frequency considering the soil effect). In Table 2 these values are included.

$c_s\,(\mathrm{m/s})$	$f_1\,(\mathrm{Hz})$	$d\,(\mathrm{m})_{\text{canc R2}}$	Train	$V_{\text{2nd res}}\,(\mathrm{km/h})$	K_1	Canc. R2
220	6.3328	16.675	A30	190.1	0.3335	Yes
inf	6.5247	16.200	A31	190.1	0.3240	Yes
220	6.3328	22.000	HSLM-A5	250.78	0.44	No
inf	6.5247	22.000	HSLM-A5	258.37	0.44	No

Table 2: Cancellation of second resonance of $12.5\,\mathrm{m}$ $f_{1,000}$ case for $c_s = \inf$ and $c_s = 220\,\mathrm{m/s}$

In Figure 10 the maximum acceleration at mid-span is represented in terms of the quotient V/d for circulating velocities in the interval $144 - 360\,\mathrm{km/h}$. Figure 10 shows that the cancellation of the second resonance indeed takes place for this bridge when the SSI effects are included, in the same way that it happens for rigid boundary conditions.

In the same Figure 10, the response of the bridge has been obtained for a second resonance caused by a different train such that the resonant velocity is not close to a cancellation condition and, therefore should not be cancelled. That is the case of the HSLM-A5 train with characteristic distance $d = 22\,\mathrm{m}$. This train excites a second resonance of the bridge fundamental mode when travelling close to $70\,\mathrm{m/s}$ $(252\,\mathrm{km/h})$ (see Table 2). This corresponds with a non-dimensional velocity of $K_1 = 0.44$ which is far from the first cancellation situation (as it can be observed in Figure 7b). Moreover, the resonant amplitude reached in the absence of soil is considerably higher than when SSI is included. As the soil has not been assigned any damping this should be related with (i) the radiation capacity of the soil and (ii) the higher level of free vibrations associated to the SS model for a $K_1 = 0.44$ value.

In Figure 11 the acceleration time history at the bridge mid-span under the HSLM-A5 circulating at $253.44\,\mathrm{km/h}$ train has been represented for infinitely rigid soil conditions and including SSI for the particular soil with $cs = 220\,\mathrm{m/s}$. From the figure it can be detected how the bridge experiences two cycles of oscillation between the passage of two pair of axles leading to a progressive increase of the resonant response. When SSI is included in the model resonance still takes place reaching lower amplitudes.

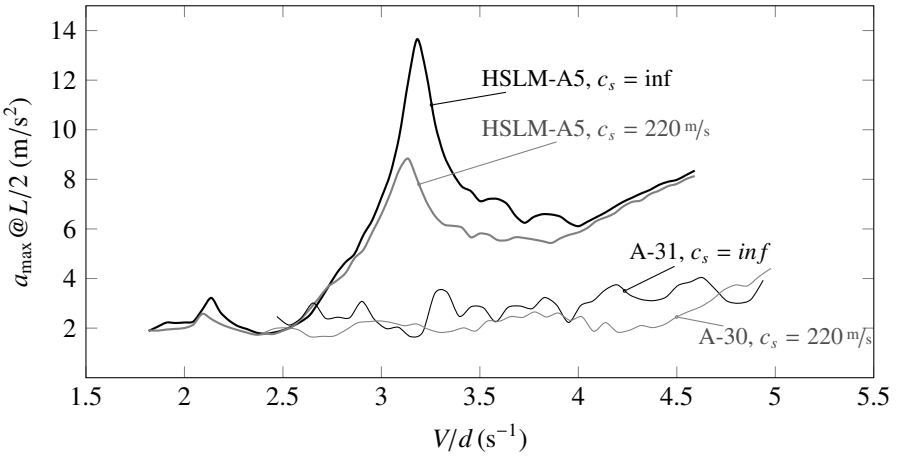

Figure 10: $a_{\max}$ vs. V/d at beam mid-span section for case $L = 12.5\,\mathrm{m}$ and $f_{1,000}$. Cancellation of second resonance of the bridge fundamental mode

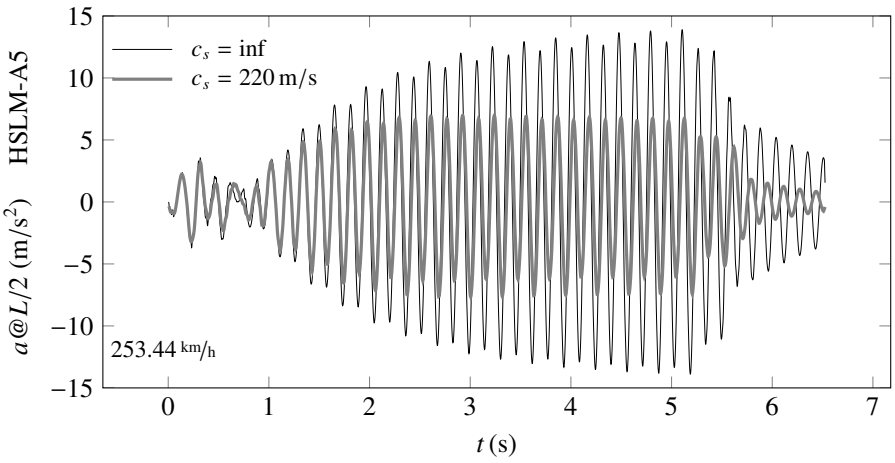

Figure 11: Acceleration time-history at beam mid-span section for HSLM-A5 at $253.44\,\mathrm{km/h}$ without SSI case and including SSI for $c_s = 220\,\mathrm{m/s}$ ($L = 12.5\,\mathrm{m}$ and $f_{1,000}$). Second resonance of bridge fundamental mode

In Figure 12 the acceleration time history at the bridge mid-span under the equidistant trains A30 and A31 circulating at 190 km/h has been represented again for infinitely rigid soil conditions and including SSI. This velocity corresponds to the velocity for cancellation of this second resonance and that explains the considerably low levels of vibration experienced by the structure.

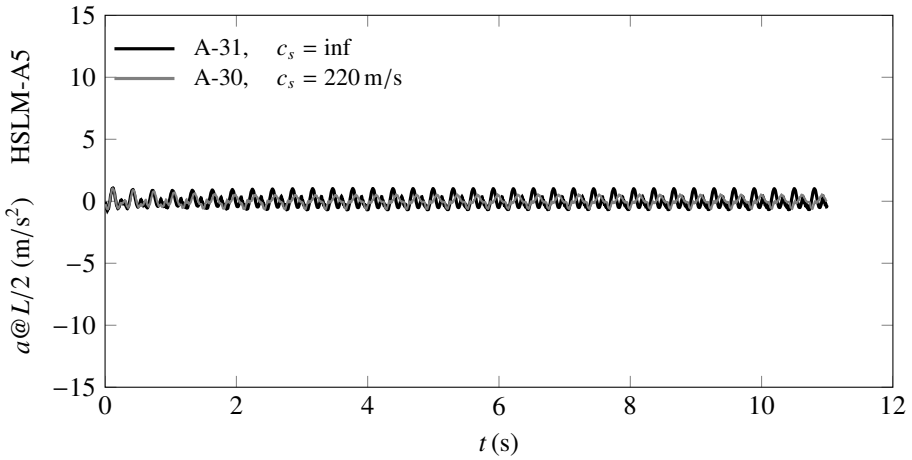

Figure 12: Acceleration time-history at beam mid-span section for HSLM-A5 at 190 km/h without SSI case and including SSI for $c_s = 220\,\mathrm{m/s}$ ($L = 12.5\,\mathrm{m}$ and $f_{1,000}$). Cancellation of second resonance of bridge fundamental mode

4.2 Influence of SSI on the bridge maximum response

Finally the effect of different soil properties is shown on the resonant amplitude of the bridge. In Figure 13 the maximum acceleration at mid-span is represented vs. the ratio V/d for the same bridge under study ($L = 12.5\,\mathrm{m}$ and $f_{1,000}$) subjected to the circulation of the HSLM-A7 train with characteristic distance $d = 24\,\mathrm{m}$. This train excites on the structure a second resonance when travelling at $282\,\mathrm{km/h}$ (condition for second resonance in the absence of SSI). As the flexibility of the soil increases, the critical velocity slightly reduces along with the structure fundamental frequency. This velocity corresponds to a value of $K_1 \approx 0.48$, associated with considerably high levels of free vibration. From Figure 7b it should be expected that the model leading to the maximum resonant response would be the one without SSI, and that the maximum acceleration response would reduce with the soil flexibility. Figure 13 shows that the bridge response aligns with this prediction and the resonant amplitude monotonically reduces with the soil flexibility.

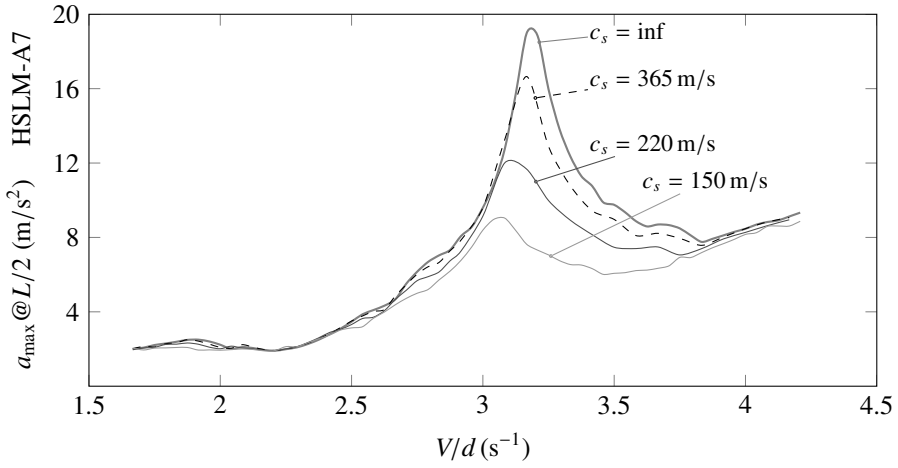

Figure 13: a_{max} vs. V/d at beam mid-span section for case $L = 12.5\,\mathrm{m}$ $f_{1,000}$. Second resonant amplitude for different soil conditions

5 Conclusions

In the present contribution, the dynamic response of beams travelled by moving loads is analyzed taking into account soil-structure interaction effects using a 3D BEM-FEM coupled numerical model integrated in the time domain. The main practical application of the study is the analysis of the transverse vibrations of simply-supported railway bridges considering short to medium span lengths. In a first approach, the fundamental frequencies of all the bridges under study are identified from the response under impulse loading. Secondly, the maximum response of the beams is obtained in the free vibration phase right after a single travelling load has crossed the structure. A wide range of circulating velocities is defined and envelopes of maximum response are obtained and analysed. From the preliminary results it is concluded that the fundamental frequency of the structures tends to the S-S one as the soil stiffness increases. The structures that are most affected by the soil flexibility are those with highest natural frequency for all the lengths. These results are consistent with the frequency evolution included in [8] for the elastically supported beam. Regarding the analysis of maximum free vibration under the circulation of single loads, it is concluded that:

- When the SSI is taken into account velocities leading to maximum free vibration response and to cancellation sequentially take place, in the same way that occurs for the E-S beam analytical case.

- As c_s and c_p decrease, going from stiffer to softer soils, the cancellation non-dimensional velocities increase as in the E-S case. This is related with the alteration in the beams natural frequencies due to the soil effect, and cancellation linear velocities remain unmodified with the flexibility of the soil.

- Depending on the non-dimensional speed interval, the maximum free vibration response may be associated to stiffer or softer soils.

- Cancellation takes place at certain speeds and the response in free vibration practically vanishes.

- When the beam transverse response is represented as a nondimensional magnitude (R) in terms of the nondimensional velocity (K_1), the maximum free vibration and cancellation conditions are practically unaffected by the beam length.

Finally the response of the bridges under study is evaluated under trains of several moving loads exciting resonant situations of the structure fundamental frequency. Through a few case studies it is shown that when resonant velocities take place close to cancellation conditions, the structural response drastically reduces and the resonant peak responses become almost imperceptible. In the same way, the amplitude of the structure at resonance varies with the soil properties following the trends observed in the free vibration analysis.

Acknowledgements

The third and fourth authors would like to acknowledge the financial support provided by the Spanish Ministry of Economy and Competitiveness (Ministerio de Economía y Competitividad) under the research project [BIA2013-43085-P].

References

[1] M. Olsson, "On the fundamental moving load problem", *Journal of Sound and Vibration*, 145(2): 299 – 307, 1991.

[2] L. Frýba, *Vibration of solids and structures under moving loads*, Thomas Telford, London, 1999.

[3] S. Law, T. Chan, Q. Zeng, "Moving Force Identification—A Frequency and Time Domains Analysis", *Journal of Dynamic Systems, Measurement, and Control*, 121: 394–401, 1999.

[4] E. Savin, "Dynamic amplification factor and response spectrum for the evaluation of vibrations of beams under successive moving loads", *Journal of Sound and Vibration*, 248(2): 267 – 288, 2001.

[5] J. Yau, Y. Yang, "Vertical accelerations of simple beams due to successive loads traveling at resonant speeds", *Journal of Sound and Vibration*, 289: 210 – 228, 2006.

[6] Y. Lu, L. Mao, P. Woodward, "Frequency characteristics of railway bridge response to moving trains with consideration of train mass", *Engineering Structures*, 42: 9 – 22, 2012.

[7] ERRI D214, *Rail bridges for speeds > 200 km/h. Final report. Part a. Synthesis of the results of D 214 research*, European Rail Research Institute, 1999.

[8] P. Museros, E. Moliner, M. Martínez-Rodrigo, "Free vibrations of simply-supported beam bridges under moving loads: Maximum resonance, cancellation and resonant vertical acceleration", *Journal of Sound and Vibration*, 332(2): 326 – 345, 2013.

[9] A. Pesterev, B. Yang, L. Bergman, C. Tan, "Revisiting the moving force problem", *Journal of Sound and Vibration*, 261(1): 75 – 91, 2003.

[10] Y. Yang, J. Yau, L. Hsu, "Vibration of simple beams due to trains moving at high speeds", *Engineering Structures*, 19(11): 936–944, 1997.

[11] Y. Yang, C. Lin, J. Yau, D. Chang, "Mechanism of resonance and cancellation for train-induced vibrations on bridges with elastic bearings", *Journal of Sound and Vibration*, 269: 345 – 360, 2004.

[12] J.R. Cho, K. Jung, K. Cho, J.W. Kwark, Y.J. Kim, B.S. Kim, "Determination of the optimal span length to minimize resonance effects in bridges on high-speed lines", *Proceedings of the Institution of Mechanical Engineers, Part F: Journal of Rail and Rapid Transit*, 2014.

[13] J. Yau, Y. Yang, S. Kuo, "Impact response of high speed rail bridges and riding comfort of rail cars", *Engineering Structures*, 9: 836–844, 1999.

[14] H. Xia, H. Li, G.D. Roeck, "Vibration Resonance and Cancellation of Simply Supported Bridges under Moving Train Loads", *Journal of Engineering Mechanics*, 140(5): 04014015, 2014.

[15] P. Museros, M. Martínez-Rodrigo, "The Cancellation Phenomenon for Simply Supported Beams and Plates subjected to Moving Loads", in B. Topping, L.C. Neves, R. Barros (Editors), *Proceedings of the Twelfth International Conference on Civil, Structural and Environmental Engineering Computing*, number Paper 48. Civil-Comp Press, Stirlingshire, UK, 2009.

[16] E. Moliner, *Dynamic behaviour of high-speed railway bridges and its retrofit with passive viscoelastic dampers*, PhD thesis, Departamento de Ingeniería de la Construcción y Proyectos de Ingeniería Civil, Universidad Politécnica de Valencia, 2012 (in Spanish).

[17] G. Mylonakis, G. Gazetas, "Seismic soil-structure interaction: beneficial or detrimental?", *Journal of Earthquake Engineering*, 04(03): 277 – 301, 2000.

[18] E. Kausel, "Early history of soil–structure interaction", *Soil Dynamics and Earthquake Engineering*, 30(9): 822 – 832, 2010, Special Issue in honour of Prof. Anestis Veletsos.

[19] M. Ülker Kaustell, R. Karoumi, C. Pacoste, "Simplified analysis of the dynamic soil–structure interaction of a portal frame railway bridge", *Engineering Structures*, 32(11): 3692 – 3698, 2010.

[20] A. Romero, M. Solís, J. Domínguez, P. Galvín, "Soil–structure interaction in resonant railway bridges", *Soil Dynamics and Earthquake Engineering*, 47: 108 – 116, 2013, SI: José Manuel Roësset.

[21] S. Ju, "Determination of scoured bridge natural frequencies with soil–structure interaction", *Soil Dynamics and Earthquake Engineering*, 55: 247 – 254, 2013.

[22] P. Galvín, A. Romero, "A {MATLAB} toolbox for soil–structure interaction analysis with finite and boundary elements", *Soil Dynamics and Earthquake Engineering*, 57: 10 – 14, 2014.

[23] P. Galvín, A. Romero, "A 3D time domain numerical model based on half-space Green's function for soil–structure interaction analysis", *Computational Mechanics*, 53: 1073–1085, 2014.

[24] S. Erhan, M. Dicleli, "Effect of dynamic soil–bridge interaction modeling assumptions on the calculated seismic response of integral bridges", *Soil Dynamics and Earthquake Engineering*, 66: 42 – 55, 2014.

[25] A. Romero, P. Galvín, J. Domínguez, "3D non-linear time domain FEM–BEM approach to soil–structure interaction problems", *Engineering Analysis with Boundary Elements*, 37(3): 501 – 512, 2013.

[26] O. Zienkiewicz, *The finite element method*, McGraw-Hill, Third edition, 1986.

[27] N. Newmark, "A method of computation for structural dynamics", *ASCE Journal of the Engineering Mechanics Division*, 85(1): 67–94, 1959.

[28] O. von Estorff, M. Prabucki, "Dynamic response in the time domain by coupled boundary and finite elements", *Computational Mechanics*, 6(1): 35–46, 1990.

[29] P. Galvín, A. Romero, J. Domínguez, "Fully three-dimensional analysis of high-speed train–track–soil-structure dynamic interaction", *Journal of Sound and Vibration*, 329(24): 5147 – 5163, 2010.

[30] European Committee for Standardization EN 1991-2, *Eurocode 1 - Actions on Structures - Part 2: Traffic loads on bridges*, CEN, Brussels, 7 2002.

[31] A. Doménech, P. Museros, M. Martínez-Rodrigo, "Influence of the vehicle model on the prediction of the maximum bending response of simply-supported bridges under high-speed railway traffic", *Engineering Structures*, 72: 123 – 139, 2014.

[32] American Association of State Highway and Transportation Officials, *AASHTO LRFD Bridge Design Specifications*, 7 2012.